NANO LETTERS

Letter

pubs.acs.org/NanoLett

Lipid Bilayer-Integrated Optoelectronic Tweezers for Nanoparticle Manipulations

Sadao Ota,[†] Sheng Wang,[†] Yuan Wang,[†] Xiaobo Yin,[†] and Xiang Zhang*[,†,‡]

[†]Department of Mechanical Engineering, University of California Berkeley, California 94720, United States

[‡]Material Sciences Division, Lawrence Berkeley National Laboratory, 1 Cyclotron Road, Berkeley, California 94720, United States

Supporting Information

ABSTRACT: Remotely manipulating a large number of microscopic objects is important to soft-condensed matter physics, biophysics, and nanotechnology. Optical tweezers and optoelectronic tweezers have been widely used for this purpose but face critical challenges when applied to nanoscale objects, including severe photoinduced damages, undesired ionic convections, or irreversible particle immobilization on surfaces. We report here the first demonstration of a lipid bilayer-integrated optoelectronic tweezers system for simultaneous manipulation of hundreds of 60 nm gold nanoparticles in an arbitrary pattern. We use a fluid lipid bilayer membrane with a ~5 nm thickness supported by a photoconductive electrode to confine the diffusion of chemically tethered nanoparticles in a two-dimensional space. Application of an external a.c. voltage together with patterned light selectively activates the photoconducting electrode that creates strong electric field localized near the surface. The field strength changes most significantly at the activated electrode surface where the particles tethered to the membrane thus experience the strongest dielectrophoretic forces. This design allows us to efficiently achieve dynamic, reversible, and parallel manipulation of many nanoparticles. Our approach to integrate biomolecular structures with optoelectronic devices offers a new platform enabling the study of thermodynamics in many particle systems and the selective transport of nanoscale objects for broad applications in biosensing and cellular mechanotransductions.

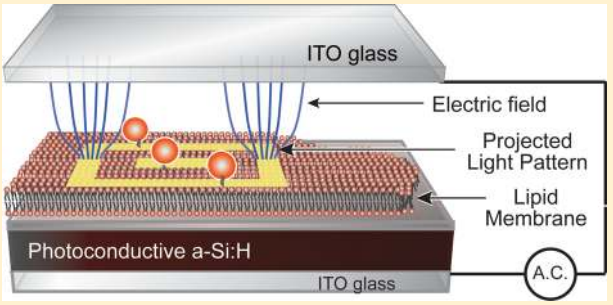

KEYWORDS: *Optical imaging, optoelectronics, supported lipid bilayer, nanoparticle, Brownian motion, soft-condensed matter physics*

Parallel manipulation of colloidal materials in noncontact manners forms the foundation in a wide range of research fields such as physics, biology,[1−5] and soft matter.[6−11] A monolayer of colloids represents analogues to various two-dimensional (2D) physical systems,[6−11] and tracking and/or controlling trajectories of these colloids allows us to study the 2D systems at the microscopic level. Especially, under an imposed potential field, the colloidal dispersion exhibits thermodynamic behaviors characteristic to many-bodied systems, offering a rich playground for understanding Brownian dynamics as well as fundamental insights into phase change behaviors such as freezing, melting, and molecular membrane dynamics.[6−11]

Parallel optical tweezers (OT) has been widely used for particle manipulation as it offers optical addressability and high resolution for trapping individual objects.[1−15] Conventionally, shaped optical fields generated with acousto-optic,[12] interference,[7] or holographic technologies[13,14] were used to form desired landscapes of the optical potential field. However, OT typically requires strong light intensity for creating a stable optical trap (>10^5 W/cm^2), which limits its application due to the potential thermal or photochemical damage to the fragile objects such as nanoparticles or biological molecules. To address this issue, the recently developed optoelectronic tweezers (OET) combined the advantage of OT with electrode-based dielectrophoresis (DEP).[16−22] In OET, light patterns were projected onto a photosensitive semiconductor substrate to form "virtual electrodes" that concentrate the electric field when an external a.c. bias is applied, in a manner similar to that of a lightning rod. The resultant nonuniform electric fields interact with the induced dipole moments in the particles and the surrounding media. This interaction results in the DEP forces, F_{OET}, expressed as the following eq 1,[23]

$$F_{OET} = 2\pi r^3 \varepsilon_m \mathrm{Re}[f_{CM}(\omega)]\nabla E_{rms}^2 \quad (1)$$

where r is the radius of spherical particles, ε_m is the relative permittivity of the medium, ∇E_{rms}^2 is the gradient of squared effective electric field, $\mathrm{Re}[f_{CM}(\omega)]$ is the real part of Clausius−Mossotti (CM) factor $f_{CM}(\omega)$ that represents the complex polarizability of the particle in the medium under the applied a.c. electric field at the angular frequency of ω. In essence, under the alternating nonuniform electric field, the particle experiences attractive or repulsive forces depending on the sign of the CM factor. The use of virtual electrodes in the OET simultaneously enables both dynamic optical addressability and

Received: March 18, 2013
Revised: May 2, 2013

dx.doi.org/10.1021/nl400999f | *Nano Lett.* XXXX, XXX, XXX−XXX

Report Documentation Page

Form Approved
OMB No. 0704-0188

1. REPORT DATE	2. REPORT TYPE	3. DATES COVERED
MAY 2013		**00-00-2013 to 00-00-2013**

4. TITLE AND SUBTITLE	5a. CONTRACT NUMBER
Lipid Bilayer-Integrated Optoelectronic Tweezers for Nanoparticle Manipulations	5b. GRANT NUMBER
	5c. PROGRAM ELEMENT NUMBER
6. AUTHOR(S)	5d. PROJECT NUMBER
	5e. TASK NUMBER
	5f. WORK UNIT NUMBER
7. PERFORMING ORGANIZATION NAME(S) AND ADDRESS(ES) **University of California at Berkeley,Department of Mechanical Engineering,Berkeley,CA,94720**	8. PERFORMING ORGANIZATION REPORT NUMBER
9. SPONSORING/MONITORING AGENCY NAME(S) AND ADDRESS(ES)	10. SPONSOR/MONITOR'S ACRONYM(S)
	11. SPONSOR/MONITOR'S REPORT NUMBER(S)

12. DISTRIBUTION/AVAILABILITY STATEMENT
Approved for public release; distribution unlimited

13. SUPPLEMENTARY NOTES

14. ABSTRACT

Remotely manipulating a large number of microscopic objects is important to soft-condensed matter physics biophysics, and nanotechnology. Optical tweezers and optoelectronic tweezers have been widely used for this purpose but face critical challenges when applied to nanoscale objects, including severe photoinduced damages, undesired ionic convections, or irreversible particle immobilization on surfaces. We report here the first demonstration of a lipid bilayer-integrated optoelectronic tweezers system for simultaneous manipulation of hundreds of 60 nm gold nanoparticles in an arbitrary pattern. We use a fluid lipid bilayer membrane with a ∼5 nm thickness supported by a photoconductive electrode to confine the diffusion of chemically tethered nanoparticles in a two-dimensional space. Application of an external a.c. voltage together with patterned light selectively activates the photoconducting electrode that creates strong electric field localized near the surface. The field strength changes most significantly at the activated electrode surface where the particles tethered to the membrane thus experience the strongest dielectrophoretic forces. This design allows us to efficiently achieve dynamic, reversible, and parallel manipulation of many nanoparticles. Our approach to integrate biomolecular structures with optoelectronic devices offers a new platform enabling the study of thermodynamics in many particle systems and the selective transport of nanoscale objects for broad applications in biosensing and cellular mechanotransductions.

15. SUBJECT TERMS

16. SECURITY CLASSIFICATION OF:			17. LIMITATION OF ABSTRACT	18. NUMBER OF PAGES	19a. NAME OF RESPONSIBLE PERSON
a. REPORT **unclassified**	b. ABSTRACT **unclassified**	c. THIS PAGE **unclassified**	**Same as Report (SAR)**	**5**	

large forces at low light intensities (~1 W/cm^2) to achieve massive manipulation of microspheres and biological cells.[16]

Despite the versatility of the OET, manipulating nanoscale objects is still a challenge because particles with smaller sizes experience weaker DEP force as the force is proportional to the particle volume (eq 1), while their Brownian motion is constantly set by thermal energy. Furthermore, nanoparticles subject to larger Brownian fluctuations can easily escape from the potential trap, since the DEP force decreases rapidly with the distance from the photoconductive channel with the decreasing gradient of the squared electric field. Efforts have been made to address this issue by operating the OET device at a lower a.c. frequency (<10 kHz), where the light-induced a.c. electro-osmosis and/or electro-thermal flow[19] was utilized to concentrate and immobilize the nanoscale objects.[24] Yet, due to the intrinsic difficulty in controlling the 3D fluidic flows and the particles' irreversible immobilization onto surfaces, the reversible manipulation of nanoscale objects still remains challenging.

In this paper, we report the first demonstration of integrating a supported lipid bilayer (SLB), an ultrathin (~5 nm) 2D fluid, with the OET for parallel manipulation of nanoparticles. The SLB continuously covers the whole photoconductive substrate and confines the motion of nanoparticles tethered to the membrane in extreme vicinity of the substrate (Figure 1a). Since the electric field strength most significantly changes near the substrate surface, the SLB integration ensures that large DEP forces can be applied onto the particles (Figure 1b). Using this approach, we have demonstrated the dynamic, reversible, and parallel manipulation of hundreds of gold nanoparticles (<60 nm) in 2D space.

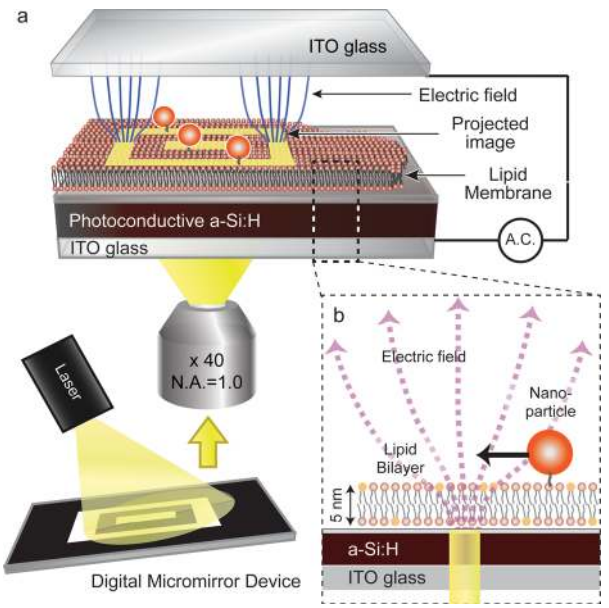

Figure 1. Optoelectronic tweezers integrated with a supported lipid bilayer (SLB). (a) Schematic of experimental setup. An aqueous solution was sandwiched between a transparent ITO electrode and a photoconductive (hydrogenated amorphous silicon) electrode. By simultaneously projecting light patterns from the DMD onto the photoconducting layer and applying an a.c. electrical bias, the photoinduced "virtual electrodes" create dielectrophoretic traps in the illuminated areas. The SLB of 5 nm thickness is formed on the silicon surface with retained lateral fluidity. (b) Due to the two-dimensional confinement imposed by the SLB, tethered particles diffuse only in lateral directions in the extreme vicinity of the photoconductive substrate surface. This configuration allows the efficient application of the light-induced DEP force to the particles because, at the photoactivated surface, the field strength changes most significantly, and the dielectrophoretic force is thus strongest.

The first step toward the final integration was to confirm the SLB formation in the OET. When properly prepared, the supported phospholipid-membrane retains the lateral fluidity, necessary for the dynamic particle manipulation. The OET device in this Letter consists of an aqueous solution sandwiched between two flat electrodes: one side is 200 nm thickness of a photoconductive hydrogenated amorphous silicon (a-Si) layer deposited on top of 100 nm of an indium tin oxide (ITO) layer, and the other side is only the 100 nm of ITO layer. Before the SLB formation on the a-Si substrate, we cleaned it with strongly oxidizing acids such that its surface was continuously covered with a thin hydrophilic silicon dioxide layer. The SLB was then formed onto this hydrophilic surface using standard vesicle fusion method.[25−27] The lipid membrane used in this experiment consisted of DOPC (1,2-dioleoyl-*sn*-glycero-3-phosphocholine, Avanti Polar Lipids, Alabaster, AL) doped with 1 mol % Oregon Green 488 DHPE (1,2-dihexadecanoyl-*sn*-glycero-3-phosphoethanolamine, Invitrogen, Carlsbad, CA).

The formation of the SLB and its maintained lateral fluidity were confirmed by fluorescence recovery after bleaching (FRAP)[28,29] under normal confocal microscopy. In the FRAP experiment, after bleaching a 10 μm spot with concentrated laser exposure, we took time-sequential fluorescence images of the membrane. The average fluorescence intensity of the bleached spots showed rapid recovery due to the lateral diffusion of fluorescent lipids within the fluid membrane (Figure 2a). By fitting this intensity curve measured from five

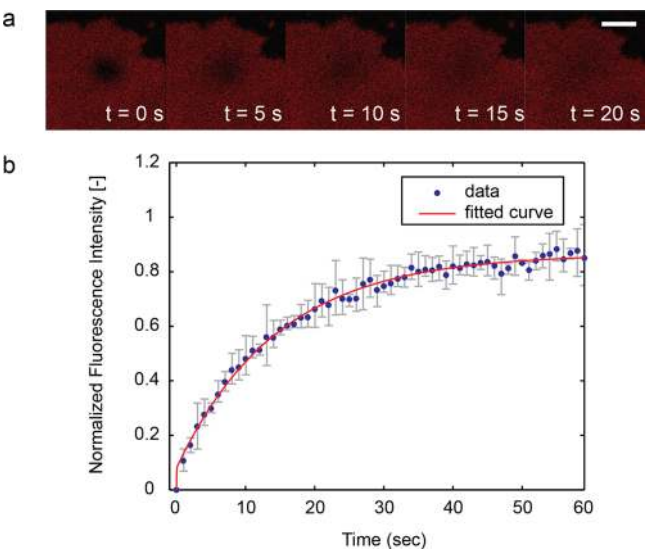

Figure 2. Fluorescence recovery after photobleaching (FRAP) experiment. (a) Time-sequential FRAP images of the SLB formed on the amorphous silicon surface, taken by normal confocal microscope. The center spot was bleached with a focused laser, and the recovery in its average fluorescence intensity was continuously monitored. The resultant rapid recovery confirmed the maintained fluidity of the SLB on the OET device. Scale bar is 20 μm. (b) Plots are the normalized average fluorescence intensity of the bleached spot versus time, showing the recovery with estimated diffusion coefficient of 8.9 μm^2/s. Here the formed SLB was a mixture of 99% DOPC and 1% of fluorescently labeled DHPE.

dx.doi.org/10.1021/nl400999f | *Nano Lett.* XXXX, XXX, XXX−XXX

samples with a theoretical curve, their diffusion coefficient was estimated as 8.9 $\mu m^2/s$ (Figure 2b, methods in the SI[30]). The measured value was very similar to the diffusivity of phospholipids on a clean glass coverslip,[31,32] confirming the maintained membrane fluidity on the fabricated a-Si surface.

We then chemically tethered the gold nanoparticles to the SLB containing thiol-ended lipids, and confirmed their confined (2D) Brownian motion. The SLB used in the following experiments consisted of 96 mol % of DOPC and 4 mol % of thiol-ended lipids, PTE-SH (1,2-dipalmitoyl-*sn*-glycero-3-hosphothioethanol, Avanti, Alabaster, AL). This PTE-SH provides thiol-anchoring groups for selectively tethering the gold nanoparticles to the SLB.[33,34]

The 2D Brownian motion of the SLB-tethered nanoparticles was optically mapped and confirmed by interferometric scattering detection, which provides sufficiently high contrast images for tracking particles' trajectories[35] (Figure 3a). Figure 3b shows the trajectories of one example particle, taken by 20 Hz for 350 frames. Continuously constant intensity of the particles in the time-lapsed images confirmed the constant distance from the reflective a-Si surface and the confinement of particles' motions on the 2D lipid membrane. The mean square displacement (MSD), obtained from 3000 frames of the trajectories of each 30 particle, showed a linear increase with slope = 1, confirming the diffusive behavior of the tethered particles. With the general law of random diffusion, $\langle \Delta r^2 \rangle = 2D\Delta t$, we calculated the lateral diffusivity of the particles from the MSD as 0.280 $\mu m^2/s$. On the other hand, the diffusivity of the same-sized particle (60 nm) in bulk water is estimated as $D = (k_B T)/(6\pi\eta r) = 7.31$ $\mu m^2/s$, wherein η is the fluid viscosity, k_B is the Boltzmann constant, and T is the room temperature at 298 K. The measured particles' diffusivity was orders smaller than that in bulk water, due to the viscous environment as well as the 2D confinement imposed by the fluid SLB.[36]

Finally, the SLB-tethered nanoparticles were successfully manipulated using the OET. The OET was operated by simultaneously applying an a. c. bias of 10 V p.p. at 100 kHz between the two ITO electrodes as well as optical illumination in the photoconductive electrode with a C.W. laser at wavelength of 594 nm. This excitation laser light was reflectively patterned to sample at intensities of ~5 W/cm^2 using a digital micromirror device (Texas Instruments, TX, USA). Figure 4a shows the overlapped image of the projected light patterns and the randomly distributed tethered gold nanoparticles of 60 nm diameters. As seen in Figure 4b and c, the OET effectively exerted the light-induced DEP forces onto the particle and move them into the light patterns (Supporting Movie 1). The histogram shown in Figure 4d shows the time evolution of the particle distribution under the OET operation, confirming the successful collection of particles toward the projected light patterns. After turning off either the applied a.c. bias or the projected light, the DEP forces disappeared, and the particles thus recovered the free (tethered) 2D Brownian

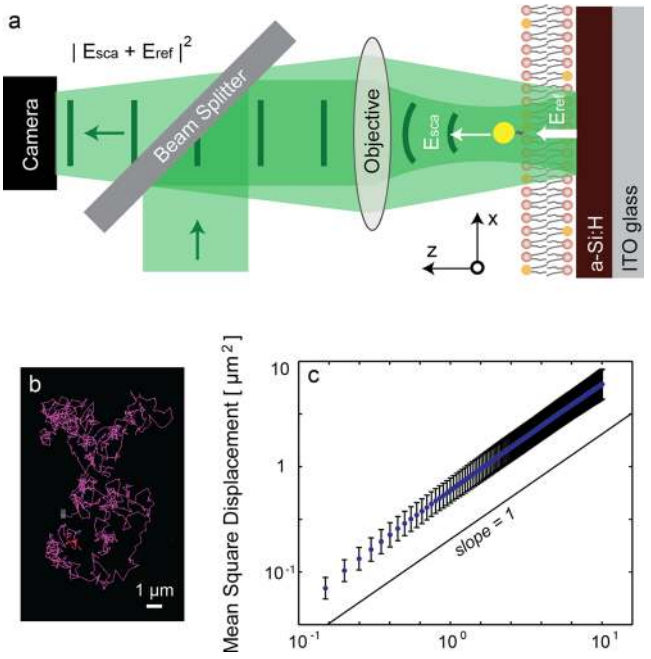

Figure 3. Two-dimensional Brownian motion of gold nanoparticles (60 nm in diameter) tethered onto the SLB/a-Si. (a) Setup for interferometric scattering detection of nanoparticle with an inverted optical microscope (not to scale). Under monochromatic illumination applied to the sample, both backscattered light from nanoparticles and reflected light from the silicon surface were collected, generating a high contrast image of the nanoparticle. (b) Long-time diffusion of the tethered nanoparticles tracked with its constant light intensity, confirming that the SLB maintained the distance between the particles and Si-surface. (c) The mean square displacement (MSD), averaged from the trajectories of the 30 tracked particles, increased linearly with time with slope = 1, confirming their diffusive behavior. The measured diffusivity calculated from the MSD was 0.28 $\mu m^2/s$. Here the formed SLB was mixture of 96 mol % of DOPC and 4 mol % of a thiol-ended lipid, PTE-SH.

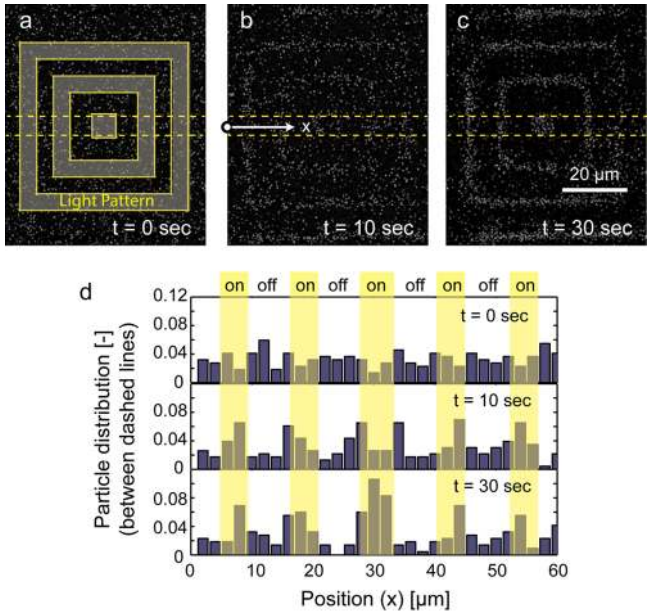

Figure 4. Manipulation of the nanoparticles tethered to the fluid SLB using the OET. Parts a–c are the time-sequence images (B/W inverted for visualization) of the gold nanoparticles, showing that they were successfully trapped into the projected light patterns. The light pattern is shown in a. After turning off either the a.c. bias or light pattern projection, the particles were released from the DEP forces and recovered the free (tethered) 2D diffusion. (d) Particle distribution under the OET operation normalized by the total number of particles in a section in each image (defined with dashed lines). The time-dependent distribution showed the successful collection of the nanoparticles into the projected light pattern.

dx.doi.org/10.1021/nl400999f | *Nano Lett.* XXXX, XXX, XXX–XXX

motion. In contrast to the low frequency operation, which may induce electro-kinetic flows and/or particle aggregation onto the a-Si surfaces, the SLB-assisted process was reversible and dynamically controllable owing to the fluidic property and the 2D confinement in the SLB.

To our knowledge, the well-controlled, reversible manipulation of nanoscale particles has been challenging for the conventional OT and OET techniques. Our approach made it possible with following advantages: (1) 2D confinement of particles' diffusion imposed by the SLB enables efficient application of the strong light-induced DEP force near the photoconductive surface; (2) the SLB prevents nonspecific and irreversible binding of the particles onto the substrate; and (3) the high viscosity of the SLB makes particle resistive to the ionic fluid flow above the electrode surface.

Simply by decreasing the frequency from 100 kHz, our configuration may allow us to manipulate even smaller particles using the electro-osmosis effect. However, we found that operating the device at frequency smaller than 20 kHz can induce instability of the supported bilayers. Continuous monitoring of the fluorescently labeled membrane showed the production of many uniform lipid vesicles from the area illuminated (see Supporting Movie 2). This is similar to a commonly known vesicle production process, electroformation.[37,38] This finding may lead to development of a new method that can generate vesicles production from targeted area in the SLB on demand.

In conclusion, we have proposed and demonstrated the integration of the supported lipid bilayer with optoelectronic tweezers, enabling 2D manipulation of many nanoparticles in desired patterns. The capability of manipulating small particles down to 60 nm diameters holds great potential in controlling many particles simultaneously for the study of various 2D physical systems and underlying Brownian mechanics. The DEP force maximized at the 2D membrane surface can be used to fractionate and/or sort the small objects with high selectivity[39−41] and to transport desired number of nanoparticles to in vitro cells as drug vehicles.[42] Moreover, since the lipid bilayer is essential components of cell membranes, the SLB has been extensively used with living cells to mimic cell-to-cell interfaces for the study of intercellular interactions.[43−45] Through the nanoparticles tethered on the SLB, our technique will facilitate the research of mechanotransductions and molecular sensing at the cellular interface.

■ ASSOCIATED CONTENT

Ⓢ Supporting Information

Methods and supporting movies. This material is available free of charge via the Internet at http://pubs.acs.org.

■ AUTHOR INFORMATION

Corresponding Author

*E-mail: xiang@berkeley.edu.

Notes

The authors declare no competing financial interest.

■ ACKNOWLEDGMENTS

The authors acknowledge funding support from the U.S. Army Research Office (ARO) MURI program (W911NF-09-1-0539) and the U.S. National Science Foundation (NSF CMMI-1120724).

■ ABBREVIATIONS

ITO, indium tin oxide:; a-Si:H, hydrogenated amorphous silicon:; DMD, digital micromirror device; SLB, supported lipid bilayer

■ REFERENCES

(1) Moffitt, J. R.; Chemla, Y. R.; Smith, S. B.; Bustamante, C. *Annu. Rev. Biochem.* **2008**, *77*, 205−228.
(2) Abbondanzieri, E. A.; Greenleaf, W. J.; Shaevitz, J. W.; Landick, R.; Block, S. M. *Nature* **2005**, *438*, 460−465.
(3) Sako, Y.; Kusumi, A. *J. Cell Biol.* **1995**, *129*, 1559−1574.
(4) Saxton, M. J.; Jacobson, K. *Annu. Rev. Biophys. Biomol. Struct.* **1997**, *26*, 373−399.
(5) Edidin, M.; Kuo, S.; Sheetz, M. *Science* **1991**, *254*, 1379−1382.
(6) Brunner, M.; Bechinger, C. *Phys. Rev. Lett.* **2002**, *88*, 248302.
(7) Chowdhury, A.; Ackerson, B. J.; Clark, N. A. *Phys. Rev. Lett.* **1985**, *55*, 833−836.
(8) Mikhael, J.; Roth, J.; Helden, L.; Bechinger, C. *Nature* **2008**, *454*, 501−504.
(9) Korda, P. T.; Grier, D. G. *J. Chem. Phys.* **2001**, *114*, 7570.
(10) Dholakia, K.; Čižmár, T. *Nat. Photonics* **2011**, *5*, 335−342.
(11) Barry, E.; Dogic, Z. *Proc. Natl. Acad. Sci. U.S.A.* **2010**, *107*, 10348−10353.
(12) Visscher, K.; Gross, S. P.; Block, S. M. *IEEE J. Quantum Electron.* **1996**, *2*, 1066−1076.
(13) Martín-Badosa, E.; Montes-Usategui, M.; Carnicer, A.; Andilla, J.; Pleguezuelos, E.; Juvells, I. *J. Opt. A: Pure Appl. Opt.* **2007**, *9*, S267−S277.
(14) Reicherter, M.; Haist, T.; Wagemann, E. U.; Tiziani, H. J. *Opt. Lett.* **1999**, *24*, 608−610.
(15) Yang, A. H. J.; Moore, S. D.; Schmidt, B. S.; Klug, M.; Lipson, M.; Erickson, D. *Nature* **2008**, *457*, 71−75.
(16) Chiou, P. Y.; Ohta, A. T.; Wu, M. C. *Nature* **2005**, *436*, 370−372.
(17) Jamshidi, A.; Pauzauskie, P. J.; Schuck, P. J.; Ohta, A. T.; Chiou, P. Y.; Chou, J.; Yang, P.; Wu, M. C. *Nat. Photonics* **2008**, *2*, 86−89.
(18) Zarowna-Dabrowska, A.; Neale, S. L.; Massoubre, D.; McKendry, J.; Rae, B. R.; Henderson, R. K.; Rose, M. J.; Yin, H.; Cooper, J. M.; Gu, E.; Dawson, M. D. *Opt. Express* **2011**, *19*, 2720−2728.
(19) Valley, J. K.; Jamshidi, A.; Ohta, A. T.; Hsu, H. Y.; Wu, M. C. *J. Microelectromech. Syst.* **2008**, *17*, 342−350.
(20) Hsu, H. Y.; Ohta, A. T.; Chiou, P. Y.; Jamshidi, A.; Neale, S. L.; Wu, M. C. *Lab Chip* **2009**, *10*, 165.
(21) Shah, G. J.; Ohta, A. T.; Chiou, E. P. Y.; Wu, M. C.; Kim, C. J. C. *Lab Chip* **2009**, *9*, 1732.
(22) Yang, S. M.; Yu, T. M.; Huang, H. P.; Ku, M. Y.; Hsu, L.; Liu, C. H. *Opt. Lett.* **2010**, *35*, 1959−1961.
(23) Tsutsui, H.; Yu, E.; Marquina, S.; Valamehr, B.; Wong, I.; Wu, H.; Ho, C. M. *Ann. Biomed. Eng.* **2010**, *38*, 3777−3788.
(24) Jamshidi, A.; Neale, S. L.; Yu, K.; Pauzauskie, P. J.; Schuck, P. J.; Valley, J. K.; Hsu, H. Y.; Ohta, A. T.; Wu, M. C. *Nano Lett.* **2009**, *9*, 2921−2925.
(25) Cremer, P. S.; Boxer, S. G. *J. Phys. Chem. B* **1999**, *103*, 2554−2559.
(26) Groves, J. T. *Science* **1997**, *275*, 651−653.
(27) Deng, Y.; Wang, Y.; Holtz, B.; Li, J.; Traaseth, N.; Veglia, G.; Stottrup, B. J.; Elde, R.; Pei, D.; Guo, A.; Zhu, X. Y. *J. Am. Chem. Soc.* **2008**, *130*, 6267−6271.
(28) Sprague, B. L.; Pego, R. L.; Stavreva, D. A.; McNally, J. G. *Biophys. J.* **2004**, *86*, 3473−3495.
(29) Axelrod, D.; Koppel, D. E.; Schlessinger, J.; Elson, E.; Webb, W. W. *Biophys. J.* **1976**, *16*, 1055−1069.
(30) Rapsomaniki, M. A.; Kotsantis, P.; Symeonidou, I. E.; Giakoumakis, N. N.; Taraviras, S.; Lygerou, Z. *Bioinformatics* **2012**, *28*, 1800−1801.
(31) Seu, K. J.; Pandey, A. P.; Haque, F.; Proctor, E. A.; Ribbe, A. E.; Hovis, J. S. *Biophys. J.* **2007**, *92*, 2445−2450.

(32) Tabarin, T.; Martin, A.; Forster, R. J.; Keyes, T. E. *Soft Matter* **2012**, *8*, 8743.
(33) Ba, H.; Rodríguez-Fernández, J.; Stefani, F. D.; Feldmann, J. *Nano Lett.* **2010**, *10*, 3006−3012.
(34) Yang, Y. H.; Nam, J. M. *Anal. Chem.* **2009**, *81*, 2564−2568.
(35) Krishnan, M.; Mojarad, N.; Kukura, P.; Sandoghdar, V. *Nature* **2010**, *467*, 692−695.
(36) Yoshina-Ishii, C.; Chan, Y. H. M.; Johnson, J. M.; Kung, L. A.; Lenz, P.; Boxer, S. G. *Langmuir* **2006**, *22*, 5682−5689.
(37) Angelova, M. I.; Dimitrov, D. S. *Faraday Discuss. Chem. Soc.* **1986**, *81*, 303.
(38) Rodriguez, N.; Pincet, F.; Cribier, S. *Colloids Surf., B* **2005**, *42*, 125−130.
(39) Xiao, K.; Grier, D. G. *Phys. Rev. Lett.* **2010**, *104*, 028302.
(40) Milne, G.; Rhodes, D.; MacDonald, M.; Dholakia, K. *Opt. Lett.* **2007**, *32*, 1144−1146.
(41) Shi, J.; Huang, H.; Stratton, Z.; Huang, Y.; Huang, T. J. *Lab Chip* **2009**, *9*, 3354.
(42) Fan, D.; Yin, Z.; Cheong, R.; Zhu, F. Q.; Cammarata, R. C.; Chien, C. L.; Levchenko, A. *Nat. Nanotechnol.* **2010**, *5*, 545−551.
(43) Groves, J. T.; Kuriyan, J. *Nat. Struct. Mol. Biol.* **2010**, *17*, 659−665.
(44) Shen, K.; Tsai, J.; Shi, P.; Kam, L. C. *J. Am. Chem. Soc.* **2009**, *131*, 13204−13205.
(45) Manz, B. N.; Groves, J. T. *Nat. Rev. Mol. Cell Biol.* **2010**, *11*, 342−352.